International Journal on Recent and Innovation Trends in Computing and Communication
ISSN: 2321-8169 Volume: 11 Issue: 10s
DOI: https://doi.org/10.17762/ijritcc.v11i10s.7656
***Article Received:** 05 June 2023 **Revised:** 27 July 2023 **Accepted:** 16 August 2023*

Robust Brain Tissue Segmentation in AD Using Comparative Linear Transformation and Deep Learning

Vunnam Asha Latha [1], Anupama Namburu[2]
[1]School of Computer Science Engineering,
VIT-AP University,
Guntur, Andhra Pradesh, India
e-mail: ashalatha.20phd7020@vitap.ac.in
[2]School of Computer Science Engineering,
VIT-AP University,
Guntur, Andhra Pradesh, India
e-mail: namburianupama@gmail.com

Abstract— As a progressive neurological disease, Alzheimer's disease (AD), if no preventative measures are taken, can result in dementia and a severe decline in brain function, making it difficult to perform basic tasks. Over 1 in 9 people suffer from dementia caused by Alzheimer's disease and require uncompensated care. The hippocampus is extracted from MRI scans of the brain via image segmentation have been useful for diagnosing Alzheimer's disease (AD).The segmentation of the CSF region in brain MRI is critical for analyzing the stages of AD. The extraction of Hippocampus from an MRI of the brain is greatly influenced by the contrast of the images. Using comparative linear transformation in the horizontal and vertical dimensions as well as statistical edge-based features, this article proposes a robust method for segmentation technique for the extraction of Hippocampus from brain MRI. These transformations aid in balancing the brain image's thin and dense fluid extractions. Through use of the ADNI dataset, the proposed approach had a 99% success rate in segmentation.

Keywords- Segmentation, Alzheimer's Disease, comparative linear transformation, Hippocampus, Cerebrospinal fluid

I. INTRODUCTION

The most common variety of dementia related to ageing is an Alzheimer's disease (AD). In most cases, the clinical presentation of AD follows a preclinical stage that is relatively free of symptoms [1]. Individuals affected with AD acquire mild cognitive impairment (MCI) [2] when the first clinical indications occur in the onset stage, which progresses to Alzheimer's disease dementia (ADD).

The CSF at these periods reflects biochemical changes occurring in the brain [4, 5]. It is well-established that decreased Cerebrospinal Fluid measurable levels of amyloid-beta 42, which is a diagnostic sign of amyloidosis and increased in tau species, which are markers of the neurofibrillary tangles and axonal damage, are diagnostic biomarkers for Alzheimer's disease [6, 7]. Mainly, it has been demonstrated that analysis of these CSF biochemical markers for Alzheimer's disease can predict conversion from MCI to ADD with an accuracy of greater than 80% [8–10]. 30-50% of MCI patients acquire ADD within 5 years, depending on their age [11]. As a result, early detection is critical for providing proper counselling to plan the treatment and care. On top of that, the ability to make early detection as a means of When evaluating the efficacy of a potential new treatment, the onset of symptoms is crucial, disease-modifying potential medications for the purpose of Medicine for Alzheimer's disease.

For better precision in Alzheimer's disease (AD) diagnoses, it's critical in order to tell apart Alzheimer's disease and the other types of dementia (non-AD). Therefore, this article aimed to summarize the data concerning the Hippocampus radius ratio's application in the Alzheimer's disease diagnosis differential dementia and foresight into the future of Alzheimer's dementia in cases with MCI.

Traditional methods for segmenting curved objects [12] concentrate focusing heavily on engineering new features to solve these issues. In order to extract features from images, filters and specialised morphological approaches are routinely employed. Finding the Hippocampal radius from MRI using these feature-based methods typically involves careful parameter tweaking and widespread implementation challenges. Long Short-Term Memory (LSTM) and Convolutional Neural Network (CNN) are the effective deep learning models that operate in tandem, with CNN detecting fluid range in images and LSTM creating image labels. The authors developed a Model for localization for deep network

International Journal on Recent and Innovation Trends in Computing and Communication
ISSN: 2321-8169 Volume: 11 Issue: 10s
DOI: https://doi.org/10.17762/ijritcc.v11i10s.7656
***Article Received:** 05 June 2023 **Revised:** 27 July 2023 **Accepted:** 16 August 2023*

using a patch-based methodology and trained the model using data from the ADNI database [13]. The classification of the CSF is performed using a neural network with radial basis functions [14]. Many AD detection algorithms evaluate, compare, and validate themselves using open source data sets comprising practical examples. True algorithmic reliability is unknown because they do not account for all parameter ranges in the data sets. In this study, Alzheimer's disease (AD) data are normal and abnormal conditions were computer-generated The three stages of Alzheimer's disease (mild, moderate, and severe) each have their own unique visual hallmarks indicating AD Degree of Severity across the entire spectrum within bounds.

Updated algorithms that employ deep learning [15,16] to divide up round things outperform their predecessors significantly. To enhance segmentation's effectiveness, These methods emphasise on primarily on the construction of diverse network architectures and loss functions. The most advanced algorithmic systems have a high degree of accuracy within the same dataset, but cannot be applied to images with varying contrasts.

This research tries to address that shortcoming by exploring how to apply deep learning to the issue of brain MRI segmentation. Our Comparative linear transformation (CLT) modification is an innovative alternative to altering the source image . Because of its contrast-insensitivity, its fluid structure can be deduced from it. Using Euclidean distance, the present pixel is compared to its neighbouring pixels' Intensity ranking in the article. Here, horizontal's and vertical's two-order transforms internal to predetermined far off are utilized to produce a resulting channel. Additionally, Statistical characteristics based on edges are generated and combined with the CLT to create an image. Without depending on a hard and fast intensity value, this encapsulates the essential characteristics of brain structure.

Any technique based on the deep learning can use CLT by substituting a distinct input CLT-transformed images serve as the input data for most recent IterNet network for deep learning, which then conducts experiment on the ADNI data to generate a potent sequence capable of locating the Hippocampus range with efficiency. This method is highly effective at capturing the characteristics of the Hippocampus range and broadening the applicability of existing techniques. The primary significance of this research is as follows:

1) An improvement to the innovative image transformation approach that thinks about the natural properties of Hippocampus range in brain MRI and is not affected by changes in image contrast.

2) Using CLT as input to a deep learning-based method makes it possible for the model to find Hippocampus range in brain MRI with better generalization.

II. RELATED WORK

The researchers hope that their methodology can speed up and lower the cost of hippocampus tissue identification for medical personnel. The goal of this study is to create a machine-readable diagnostic tool for identifying abnormal Hippocampus radius from brain MRI scans as quickly as possible.

A. Alzheimer's impact on Brain Tissues

Alzheimer disease (AD) is mostly diagnosed neural organ The hippocampus, a brain area whose atrophy is linked to the development of Alzheimer's disease and other forms of dementia, is extracted using segmentation from MRI images in the ADNI dataset. Numerous investigations have demonstrated that the CSF pattern in Alzheimer's is characterized by an increase in t-Tau and p-Tau and a decrease in Aβ1-42[17-19]. Additionally, there have been studies that the amount of CSF affects the significance of Aβ1-42 peptides [20], and consideration may help to reduce this bias [21,22]. Explanation of the healthy brain and Alzheimer's brain is shown in the Fig.1. The course of Alzheimer's disease tends to steadily through 3 stages: early, middle, and late (sometimes referred to in medical contexts as mild, moderate, and severe). As Alzheimer's affects individuals differently, dementia symptoms and progression through the stages may vary from person to person. In figure.1, we are clearly observed that the hippocampus shrinks severely due to the increase in CSF fluid.

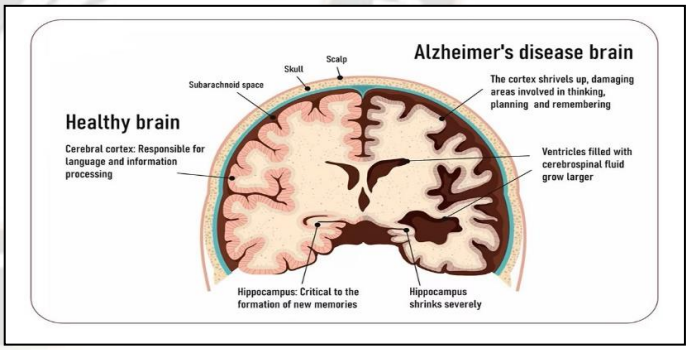

Fig.1 Hippocampus shrinks severely in Alzheimer's disease brain.

B. Deep Learning models for AD detection

Segmentation of brain tissues plays a crucial for diagnosis of AD and the patient's current stage of AD. The extraction of tissues from brain MRI was always difficult due to the resemblance of morphology at random brain locations. Statistical segmentation of the tissues is essential for assessing shapes and angles and detecting other brain-related diseases via accurate brain MRI segmentation. For example, clearly show

International Journal on Recent and Innovation Trends in Computing and Communication
ISSN: 2321-8169 Volume: 11 Issue: 10s
DOI: https://doi.org/10.17762/ijritcc.v11i10s.7656
***Article Received:** 05 June 2023 **Revised:** 27 July 2023 **Accepted:** 16 August 2023*

that hypertensive those afflicted patients suffered from reduced tilt of the cerebral cortexes.

In order to conduct quantitative examinations of Large-scale brain tissue investigations volume inside the skull in MRI, reliable Brain Segmentation robots components like GM, WM, and CSF is required as shown in figure 2. The healthy brain tissues are shown in row 1 and the Alzheimer tissues are shown in row 2 and 3. On comparing the tissues, the gray matter and CSF is increased in the Alzheimer tissues and unevenly distributed and there is a shrink in white matter.

Two popular approaches to segmenting brain tissue are atlas-based methods and pattern recognition algorithms. Atlas-based techniques [23-26] compare a target image's intensity data to that of an atlas. Despite the fact that atlas-based and registration methods commonly used for segmenting human brains [27-29], they do not produce trustworthy outcomes because of registration for small and extremely changeable tissues like the hippocampus constraints and unpredictability in the ground truth dataset. Algorithms for recognising patterns brain tissues are frequently classified using a set of local intensity characteristics [30,31]. Hippocampal having atrophy is recently been postulated as an AD biomarker [32,33]. The hippocampus is a limbic system component made up of many types of tissue. Several investigations have shown that Alzheimer's disease patients have a reduced hippocampus volume [34,35]. To identify regions with fluid activity, Shi et al. [36] advocated use local intensity transformation when the image contrast is low. Numerous characterising features and picture Methods based on enhancement were also proposed in the scientific publications for brain tissue extraction using deep learning. Nonetheless, the models must be reliable in variable settings and the extract region in less time. During enhancement of deep learning models for brain MRI segmentation data enhancement, model development, and training are only few of the factors considered.

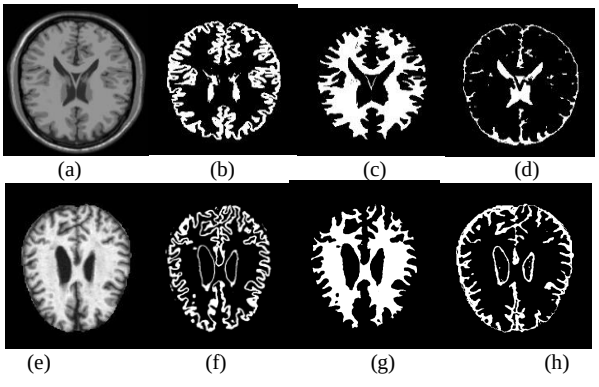

Fig. 2: The Healthy brain tissues (a) Brain MRI (b) Gray matter (c) White matter (d) CSF (row1). The AD brain tissues (e) Brain MRI (f) Gray matter (g) White matter (h) CSF (row2).

1. Data Augmentation of MRI images

When the network's complexity is too high to guarantee translucency and repeatability, deep learning's implicit bias can be difficult to adjust. Perhaps the problem is answered by collecting and analysing massive amounts of neuroimaging data the connections between feature extraction and deep learning [37]. Data augmentation is one such technique to increase the images. The following are the ways in which the data is augmented. Firstly, random rotation between -180 and 180 degrees was applied to all images and then apply the shearing with the angle between -0.1 to 0.1. After completing that shearing process, we are going to the image Flipping. In the Image Flipping horizontals and vertical's axes were flipped. And then Zoom the images and Cropping is applied for the processed images.

III. PROPOSED METHODOLOGY

Unfortunately, deep learning isn't the answer to everything. Data formats, such as those used in neuroimaging and genetics, might be challenging for deep learning methods that extract properties straight from the input data without preprocessing for feature selection. When extra input data is introduced into a closed network, it leads to confusion and ambiguity since the weights for the incoming data are automatically adjusted. In contrast, a hybrid method combines the findings of machine learning and deep learning separately on the extra data and the neural pictures, respectively.

In this article, a novel procedure for extracting features of the brain and combined with comparative linear transform and then the image classification deep learning model. Additionally, statistical edge-based feature extraction and multinomial sub-image histogram equalisation are added to improve image quality. First the image is converted into grayscale and then the histogram equalization is conducted. The edge-based statistical features that produce a single channel image and the comparative linear transformation that produces Using a two-channel picture, we can get a three-channel picture. Using the U-Net deep learning model used to remove the remaining CSF derived from improved images through previous procedures. The suggested technique is assessed in light of several variable metrics for success, including 'accuracy', 'specificity', 'sensitivity', 'precision', 'F1-score', and area under the curve. Figure 3 below depicts the proposed methodology's flowchart.

International Journal on Recent and Innovation Trends in Computing and Communication
ISSN: 2321-8169 Volume: 11 Issue: 10s
DOI: https://doi.org/10.17762/ijritcc.v11i10s.7656
***Article Received:** 05 June 2023 **Revised:** 27 July 2023 **Accepted:** 16 August 2023*

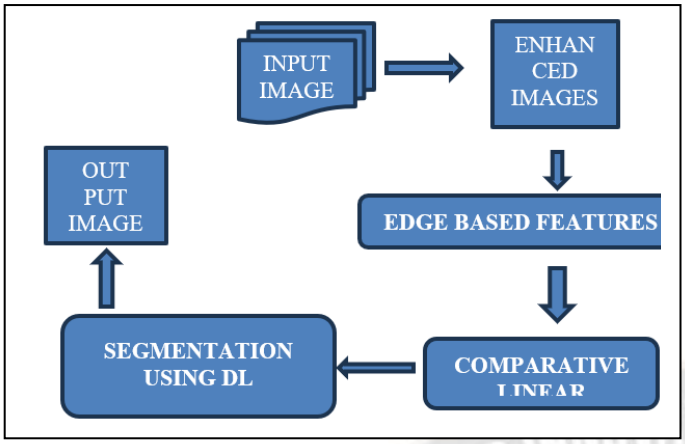

Fig. 3: Proposed Method for the Brain Tissue extraction

A. Pre-processing and Data Augmentation

1. Pre-processing

As preprocessing image histogram is applied with the goal of solving the issue of robust learning in the variance with contrast present. In addition to varying compare and contrast, A good model should be able to efficient use of tissue. Hence, combining statistical edge characteristics with CLT is useful for the extraction of features that aid in the extraction of generalized features, thereby facilitating robust learning.

2. Sub-image histogram improvement based on exposure

The Best Possible Image Quality, the "Histogram Equalisation" method standardises the image's histogram. To preserve local contrast without degrading the image's overall quality to the human eye, histogram equalization increases local luminosity and contrast. Many advance models of histogram-based image enhancement techniques are available in the literature [39]. However, on applying different models the basic histogram model is suitable for ADNI dataset.

3. Statistical Edge features

The enhanced image is further processed for statistical edge features, here the horizontal, vertical and diagonal features are used with 5*5 kernel size to extract the edge features of the image. These filters are very effective in extracting the thin vessels of the tissues. The following statistical edge features are applied on the image.

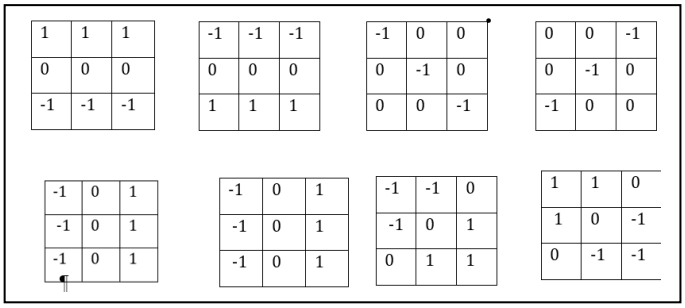

Fig. 4: Different edge filters used to extract the edges in the image

All the filters in figure 4 are applied on the histogram enhance image and then and edge filtered image is generated.

4. Comparative Linear transformations

Some of the local transformations techniques based on the Census transformation (CT) that can be found in the literature [38]. Deep learning models can benefit greatly from the extracted generalised characteristics that LIOT excels at obtaining. As a result, a network can be fed a four-channel picture for segmentation.In order to increase the efficacy of paradigm, channel generation is accomplished with the aid of edge detection filters, and two-channel rather than four-channel images are produced with the aid of a modified LIOT. The segmentation network is then supplied the three-dimensional picture with its defining edges and Two-channel pictures based on a variant of LIOT. Proposed CLT takes relative values into account rather than absolute values, resulting in a more robust method for locating the CSF region in brain images with different contrasts.

Each pixel 'P' in the image is compared to its neighbours in the vertical and horizontal directions, for a total of 14 pixels in the vertical channel and 14 pixels in the horizontal channel (7 pixels on the left and 7 pixels on the right). Each pixel is compared to its 14 neighbours $\{x_m^n, n=1, 2 ..., 14\}$, m = {v, h} where v is the vertical Euclidean distance shown with blue color in figure 5 where h is the perpendicular horizontal Euclidean distance to point P shown in blue color in fig 5. Equation 1 is used to derive the corresponding two channel output image.

$$f_m{}^1(p) = \sum_{n=-7}^{7} [f(p) > f(x^n)] * 2^{n-1} \quad (1)$$

Where $[f(P)>f(x^n)]$ is 1 if the value f(p) is larger than $f(x^n)$ the center pixel, otherwise 0. According to the first equation, the proposed CLT resilient to variations in image contrast, as it uses the local intensity gradient to spot blacked-out pixels. Therefore, offering a superior version for the generalized detection of the CSF region.

International Journal on Recent and Innovation Trends in Computing and Communication
ISSN: 2321-8169 Volume: 11 Issue: 10s
DOI: https://doi.org/10.17762/ijritcc.v11i10s.7656
***Article Received:** 05 June 2023 **Revised:** 27 July 2023 **Accepted:** 16 August 2023*

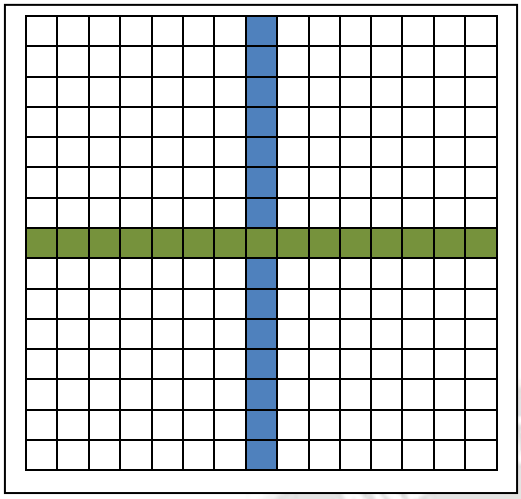

Fig.5. Proposed CLT transform

5. Division of the infrastructure of networks

To build a network that can compete using cutting-edge methods is not the goal of the suggested approach, as the model's primary objective is to improve the generalisation of methods currently used in deep learning. The signal input of IterNet is altered in in the hope of receiving the improved picture that enhanced image offers. We updated IterNet [40] to incorporate the edge and CLT image enhancements. Iternet is a three micro U-Net combination that utilises U-Net as is similar to an encoder-decoder model in terms of its base module, which to U-Net. Each tiny U-Net, which has fewer parameters than U-Net, utilizes its ancestor module's feature maps.

B. Purpose of Training

The brain MRI is segmented using the network shown in the slice. The IterNet loss serves a similar function. The network parameters for segmentation are optimized using the sigmoid cross entropy loss formula (2).

$$Q = \sum(-f_n log(P_(f_n) - (1 - f_n) log(1 - P_(f_n)) \quad (2)$$

Here, f_n represents a 0 or 1, depending on whether the pixel is part of the reference image or not, $P_{(fn)}$ is a measure of how likely it is that pixel n in the input image will have intensity. During testing, the network is fed images transformed using a multinomial image enhancement algorithm and a linear transformation feature comparison.

IV. EXPERIMENTS

The frequently employed data set— The proposed method is being tested at the moment using ADNI. When it comes to Section 4.1, a concise in brief the data set key indicators of performance employed are presented. Afterwards, targeted application details are illustrated in Section 4.2. Two distinct types of experiment proposed CLT is evaluated for its applicability in the real world: An analysis of Section 4.3 is demonstrated that the suggested border and CLT in no way significant degrade how well the first pictures worked; Comparison of image quality to demonstrate that CLT is less sensitive to changes in contrast.

A. Metrics for evaluation and data sets

We extract 20 MRIs from the ADNI, of which ten are used for training and ten for testing. The volumes of the data set are displayed in Table 1. Images of round objects at various resolutions may reveal a range in their apparent depth. To resolve inequality of proportion between the extent of one's peripheral vision and the image size, the scale in order to achieve uniformity between the images. The size of the data remains unchanged as pictures are resized from 999x960 to 584x561 These dimension values are utilized by both the reference and suggested methods.

Quantitative comparisons of segmentation findings to the truth are made using segmentation accuracy(seg_acc), sensitivity, specificity, precision, dice_coefficients, and F1-score as performance measurements. The SA, SEN, SPE, AUC, and F1-score are derived by calculating the proportion of correct predictions, incorrect predictions, and false positives and false negatives, respectively.

Table I: Data Set used for the BRAIN tissue Extraction

Dimension	Data Set	Number of images	Images for testing	Images for training	Size of the image
2D	Very Mild	20	10	10	565*584
2D	Mild	20	10	10	565*584
2D	Moderate	20	10	10	565*584

B. Particulars of the Execution

Tools for augmenting data are necessary for the sake of silence MRI datasets and visuals of different sizes. Our primary objective is to examine the generalizability of unchanging procedure to comparison, and not to construct superior performance compared to other approaches. In this case, CLT is integrated with IterNet [40], the most recent version of the latter. The entropy loss function during network training in the course of 200 iterations, with each iteration consisting of 32 elements. An Adam optimizer with a 0.001-rate learning is used to fine-tune the network. The CLT is implemented using an eight-step stride with image overlap.

International Journal on Recent and Innovation Trends in Computing and Communication
ISSN: 2321-8169 Volume: 11 Issue: 10s
DOI: https://doi.org/10.17762/ijritcc.v11i10s.7656
***Article Received:** 05 June 2023 **Revised:** 27 July 2023 **Accepted:** 16 August 2023*

C. The Outcome of Experiments

The enhancement of the picture is evaluated in the first experiment. Exposure base sub histogram clip enhancement is performed on an input image converted to grayscale. In addition, the extracted edge features and CLT of the images are shown in final outcome. The following outcome demonstrates that a focus on edges and a two-channel approach comparative linear transformation preserve region-specific information despite varying input image contraction.

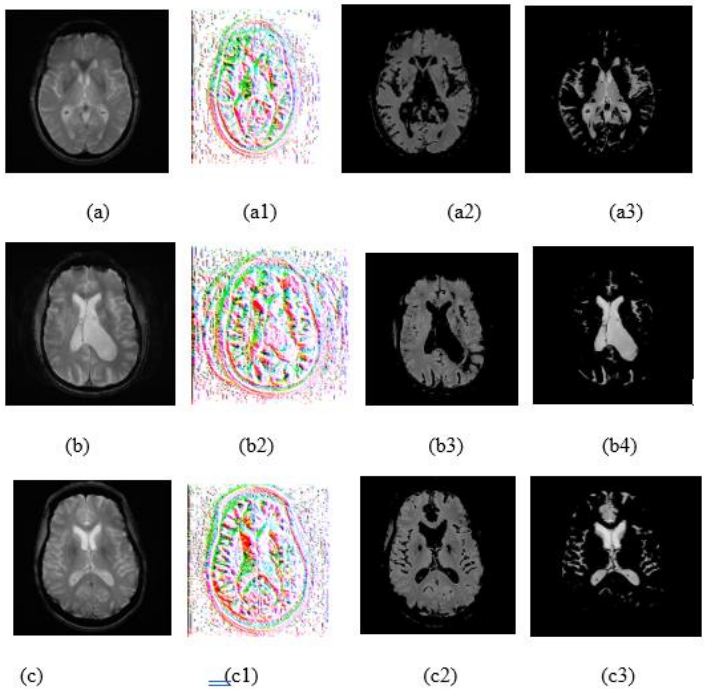

Fig. 4 : The first row named as a's represents the mild stage with training, CLT image, segmented WM, segmentation of hippocampus region using proposed one. the 2nd row represents the moderate with the same sequence and the 3rd row represents severe stage of AD.

Additionally, Aims of the Experiment validate Hippocampus region extraction from the images. Figure 4 depicts the ADNI training25 image and its CLT image, extracted utilizing the proposed method. On the surface, the separation of Hippocampus region is efficiently derived using the proposed model, and how well the original pictures worked is not materially degraded.

Table II: Assessing the effectiveness of the suggested approach.

Images	**Precision**	**Sensitivity**	**Specificity**	**Seg_acc**	**Dice_ coefficient**	**F1_score**
MILD DATA SET						
04 test imagess	0.8457	0.8146	0.9805	0.9628	0.8271	0.82502
05 test images	0.7789	0.8387	0.9763	0.9721	0.822	0.808279
06 test images	0.7771	0.8571	0.9734	0.9525	0.8219	0.810042
Average of 40 images	0.77	0.82	0.96	0.95	0.83	0.8
MODERATE DATA SET						
01 test images	0.8641	0.8821	0.9977	0.9971	0.9371	0.883107
05 test images	0.8766	0.9877	0.9951	0.9961	0.9432	0.938868
Average of 20 images	0.86	0.94	0.99	0.99	0.91	0.9
SEVERE DATA SET						
01 test images	0.7514	0.8411	0.9221	0.8935	0.711	0.909138
08 test images	0.85	0.8756	0.8611	0.832	0.9268	0.732711
Average of 20 images	0.74	0.84	0.88	0.86	0.88	0.86

International Journal on Recent and Innovation Trends in Computing and Communication
ISSN: 2321-8169 Volume: 11 Issue: 10s
DOI: https://doi.org/10.17762/ijritcc.v11i10s.7656
***Article Received:** 05 June 2023 **Revised:** 27 July 2023 **Accepted:** 16 August 2023*

The suggested method does a good job of dealing with the problems of deep learning, such as a paucity of data sets, by utilizing an augmentation technique, balancing the noise using alterations to the boundary and relative intensity order, and robustly extracting regions that are insensitive to image contrast. Table 2 displays the proposed method's "seg_acc", "sensitivity", "specificity", "precision", "dice_coefficient", and "f1score". The table displayed the individual image measurements for the both the ADNI data set and the data set's mean values. The success of the proposed approach on ADNI data was 99 percent. On the given data set, the "precision", "sensitivity", "specificity", "dice coefficient", and "f1 score" indicate excellent performance. In addition, the show or play the analysis of the suggested model is contrasted to the performance evaluation of two other recent models, IterNet[40] and LIOT [36]. Compared to these models, the proposed models' performance, the proposed model's performance has not deteriorated, and it has demonstrated comparable performance to LIOT shown in the table 3. In this table we calculate the only one image among the three datasets.

Table III: Comparison between the proposed model and traditional models

Data Set	Method	Sensitivity	Specificity	Seg_accuracy	F1-score
Mild	IterNet[40]	0.828	0.973	0.954	0.821
	LIOT[36]	0.811	0.974	0.953	0.814
	Proposed	**0.828**	**0.975**	**0.9608**	**0.816**
Moderate	IterNet[40]	0.633	0.899	0.875	0.477
	LIOT[36]	0.788	0.977	0.96	0.776
	Proposed	**0.95**	**0.989**	**0.99**	**0.981**
Severe	IterNet[40]	0.738	0.878	0.854	0.773
	LIOT[36]	0.852	0.854	0.812	0.824
	Proposed	**0.932**	**0.972**	**0.874**	**0.878**

V. CONCLUSION

This research seeks to improve the generalization capabilities of extant brain MRI segmentation techniques based on deep learning. Along with statistical edge-based characteristics, a comparative linear that which transforms utilized to determine pixels' local relativity. This method balances the cacophony, which facilitates efficient sub-grouping i.e., segmentation. In addition, we need to deal with the problem of skewed statistics, the data set is augmented using augmentation techniques. In the proposed algorithm, converted images collected with were utilised to build a deep learning model called IterNet comparative linear transformation and statistics of a border. As an alternative to, the proposed model is create a robust segmentation algorithm, i.e., one with contrast invariance like LIOT. Moreover, since the proposed model was ineffective on the Severe data set, further research should be conducted on more complex algorithms for CSF segmentation accuracy.

REFERENCES

[1] Sperling RA, Aisen PS, Beckett LA, et al. "Toward defining the preclinical stages of Alzheimer's disease: recommendations from the National Institute on Aging-Alzheimer's Association workgroups on diagnostic guidelines for Alzheimer's disease". Alzheimers Dement.2011;7:280–92.

[2] Albert MS, DeKosky ST, Dickson D, et al. "The diagnosis of mild cognitive impairment due to Alzheimer's disease: recommendations from the National Institute on Aging-Alzheimer's Association workgroups on diagnostic guidelines for Alzheimer's disease". Alzheimers Dement. 2011;7:270–9.

[3] McKhann GM, Knopman DS, Chertkow H, et al. "The diagnosis of dementia due to Alzheimer's disease: recommendations from the National Institute on Aging and the Alzheimer's Association workgroup". Alzheimers Dement. 2011;7(3):263–9.

[4] Peskind ER, Riekse R, Quinn JF, et al. "Safety and acceptability of the research lumbar puncture". Alzheimer Dis Assoc Disord. 2005;19(4):220–5.

[5] Lewczuk P, Riederer P, O'Bryant SE, et al. "Cerebrospinal fluid and blood biomarkers for neurodegenerative dementias: an update of the Consensus of the Task Force on Biological Markers in Psychiatry of the World Federation of Societies of Biological Psychiatry." World J Biol Psychiatry. 2017: 1–85. https://doi.org/10.1080/15622975.2017.1375556 [Epub ahead of print].

[6] Fagan AM, Perrin RJ. "Upcoming candidate cerebrospinal fluid biomarkers of Alzheimer's disease". Biomark Med. 2012;6(4):455–76.

International Journal on Recent and Innovation Trends in Computing and Communication
ISSN: 2321-8169 Volume: 11 Issue: 10s
DOI: https://doi.org/10.17762/ijritcc.v11i10s.7656
***Article Received:** 05 June 2023 **Revised:** 27 July 2023 **Accepted:** 16 August 2023*

[7] Lewczuk P, Kornhuber J. "Neurochemical dementia diagnostics in Alzheimer's disease: where are we now and where are we going?" Expert Rev Proteomics. 2011;8(4):447–58.

[8] Hampel H, Burger K, Teipel SJ, et al." Core candidate neurochemical and imaging biomarkers of Alzheimer's disease". Alzheimers Dement. 2008;4:38–48.

[9] Hansson O, Zetterberg H, Buchhave P, et al. "Association between CSF biomarkers and incipient Alzheimer's disease in patients with mild cognitive impairment: a follow-up study". Lancet Neurol. 2006;5:228–34.

[10] Mattsson N, Zetterberg H, Hansson O, et al. 'CSF biomarkers and incipient Alzheimer disease in patients with mild cognitive impairment'. JAMA. 2009; 302:385–93.

[11] Petersen RC." Mild cognitive impairment as a diagnostic entity". J Intern Med. 2004;256(3):183–94.

[12] O. Merveille, B. Naegel, H. Talbot, N. Passat, *n* d "variational restoration of curvilinear structures with prior-based directional regularization", IEEE Transactions on Image Processing 28 (8) (2019) 3848– 3859.

[13] Gao F et al (2022) "A combination model of AD biomarkers revealed by machine learning precisely predicts Alzheimer's dementia: China Aging and Neurodegenerative Initiative (CANDI) study". Alzheimers Dement. https://doi.org/10.1002/alz. 12700

[14] S. Kumar, A. Adarsh, B. Kumar, A. K. Singh, "An automated early diabetic retinopathy detection through improved blood vessel and optic disc segmentation", Optics & Laser Technology 121 (2020) 105815

[15] A. Mosinska, M. Koziński, P. Fua, "Joint segmentation and path classification of curvilinear structures", IEEE transactions on pattern analysis and machine intelligence 42 (6) (2019) 1515–1521.

[16] J. Xie, L. Fang, B. Zhang, J. Chanussot, S. Li, "Super resolution guided deep network for land cover classification from remote sensing images", IEEE Transactions on Geoscience and Remote Sensing 60 (2021) 1–12

[17] K. Blennow, H. Hampel, M. Weiner, H. Zetterberg, "Cerebrospinal fluid and plasma biomarkers in Alzheimer disease", Nat. Rev. Neurol. 6 (2010) 131–144, https://doi. org/10.1038/nrneurol.2010.

[18] P. Lewczuk, P. Riederer, S.E. O'Bryant, M.M. Verbeek, B. Dubois, P.J. Visser, K.A. Jellinger, S. Engelborghs, A. Ramirez, L. Parnetti, C.R. Jack, C.E. Teunissen, H. Hampel, A. Lleó, F. Jessen, L. Glodzik, M.J. de Leon, A.M. Fagan, J.L. Molinuevo, W.J. Jansen, B. Winblad, L.M. Shaw, U. Andreasson, M. Otto, B. Mollenhauer, J. Wiltfang, M.R. Turner, I. Zerr, R. Handels, A.G. Thompson, G. Johansson, N. Ermann, J.Q. Trojanowski, I. Karaca, H. Wagner, P. Oeckl, L. van Waalwijk VanDoorn, M. Bjerke, D. Kapogiannis, H.B. Kuiperij, L. Farotti, Y. Li, B.A. Gordon, S. Epelbaum, S.J.B. Vos, C.J.M. Klijn, W.E. Van Nostrand, C. Minguillon, M. Schmitz, C. Gallo, A. Lopez Mato, F. Thibaut, S. Lista, D. Alcolea, H. Zetterberg, K. Blennow, J. Kornhuber, "Cerebrospinal fluid and blood biomarkers for neurode- generative dementias: an update of the consensus of the task force on biological markers in psychiatry of the world federation of societies of biological psychiatry", World J. Biol. Psychiatry 19 (2018) 244–328, https://doi.org/10.1080/15622975. 2017.1375556.

[19] S. Janelidze, H. Zetterberg, N. Mattsson, S. Palmqvist, H. Vanderstichele, O. Lindberg, D. Van Westen, E. Stomrud, L. Minthon, K. Blennow, "CSF Ab42/Ab40 and Ab42/Ab38 ratios: better diagnostic markers of Alzheimer disease", Ann. Clin. Transl. Neurol. (3) (2016) 154–165, https://doi.org/10.1002/acn3.274

[20] Ana Oliveira, Yosef Ben-David, Susan Smit , Elena Popova, Milica Milić. Machine Learning for Decision Optimization in Complex Systems. Kuwait Journal of Machine Learning, 2(3). Retrieved from http://kuwaitjournals.com/index.php/kjml/article/view/201

[21] J. Toombs, R.W. Paterson, M.P. Lunn, J.M. Nicholas, N.C. Fox, M.D. Chapman, J.M. Schott, H. Zetterberg, "Identification of an important potential confound in CSF AD studies: Aliquot volume", Clin. Chem. Lab. Med. 51 (2013) 2311–2317, https:// doi.org/10.1515/cclm-2013-0293.

[22] C. Gervaise-Henry, G. Watfa, E. Albuisson, A. Kolodziej, B. Dousset, J.L. Olivier, T.R. Jonveaux, C. Malaplate-Armand, "Cerebrospinal fluid Aβ42/Aβ40 as a means to limiting tube- and storage-dependent pre-analytical variability in clinical setting", J. Alzheimers Dis. 57 (2017) 437–445, https://doi.org/10.3233/JAD-160865.

[23] E. Willemse, K. van Uffelen, B. Brix, S. Engelborghs, H. Vanderstichele, C. Teunissen, "How to handle adsorption of cerebrospinal fluid amyloid β (1–42) in laboratory practice? Identifying problematic handlings and resolving the issue by use of the Aβ42/Aβ40ratio", Alzheimers Dement. 13 (2017) 885–892, https://doi.org/10.1016/j.jalz.2017.01.010.

[24] Srhoj-Egekher, V.; Benders, M.; Viergever, M.A.; Išgum, I. "Automatic neonatal brain tissue segmentation with MRI". SPIE Med. Imaging 2013, 8669, 86691K. [CrossRef]

[25] Anbeek, P.; Išgum, I.; Van Kooij, B.J.M.; Mol, C.P.; Kersbergen, K.J.; Groenendaal, F.; Viergever, M.A.; De Vries, L.S.; Benders, M. "Automatic Segmentation of Eight Tissue Classes in Neonatal Brain MRI." PLoS ONE 2013, 8, e81895. [CrossRef]

[26] Ashraf Dhannon Hasan, Abbas Salim Kadhim, Mustafa A. Ali. (2023). Medical Image Compression Using Hybrid Compression Techniques. International Journal of Intelligent Systems and Applications in Engineering, 11(4s), 634–648. Retrieved from https://ijisae.org/index.php/IJISAE/article/view/2741

[27] Vrooman, H.; Cocosco, C.; Lijn, F.; Stokking, R.; Ikram, M.; Vernooij, M.; Breteler, M.; Niessen, W.J. "Multi-spectral brain tissue segmentation using automatically trained k-nearestneighbor classification". NeuroImage 2007, 37, 71–81. [CrossRef] [PubMed]

[28] Makropoulos, A.; Gousias, I.S.; Ledig, C.; Aljabar, P.; Serag, A.; Hajnal, J.V.; Edwards, A.D.; Counsell, S.; Rueckert, D. "Automatic Whole Brain MRI Segmentation of the Developing Neonatal Brain", IEEE Trans. Med. Imaging 2014, 33, 1818–1831. [CrossRef] [PubMed]

[29] Christensen, G.E.; Rabbitt, R.D.; Miller, M.I. "Deformable templates using large deformation kinematics." IEEE Trans. Image Process. 1996, 5, 1435–1447. [CrossRef]

International Journal on Recent and Innovation Trends in Computing and Communication
ISSN: 2321-8169 Volume: 11 Issue: 10s
DOI: https://doi.org/10.17762/ijritcc.v11i10s.7656
***Article Received:** 05 June 2023 **Revised:** 27 July 2023 **Accepted:** 16 August 2023*

[30] Davatzikos, C.; Prince, J. "Brain image registration based on curve mapping". In Proceedings of the IEEE Workshop on Biomedical Image Analysis, Seattle, WA, USA, 24–25 June 1994; pp. 245–254.

[31] Carmichael, O.T.; Aizenstein, H.J.; Davis, S.W.; Becker, J.T.; Thompson, P.M.; Meltzer, C.C.; Liu, Y. "Atlas-based hippocampus segmentation in Alzheimer's disease and mild cognitive impairment". NeuroImage 2005, 27, 979–990. [CrossRef]

[32] Wang, L.; Gao, Y.; Shi, F.; Li, G.; Gilmore, J.; Lin, W.; Shen, D. Links: "Learning-based multi-source integration framework for segmentation of infant brain images". NeuroImage 2014, 108, 734–746.

[33] Chi¸ta, S.M.; Benders, M.; Moeskops, P.; Kersbergen, K.J.; Viergever, M.A.; Išgum, I. "Automatic segmentation ˇ of the preterm neonatal brain with MRI using supervised classification". SPIE Med Imaging 2013, 8669, 86693.

[34] Cuingnet, R.; Gerardin, E.; Tessieras, J.; Auzias, G.; Lehéricy,S.; Habert, M.-O.; Chupin, M.; Benali, H.; Colliot, O. "Automatic classification of patients with Alzheimer's disease from structural MRI: A comparison of ten methods using the ADNI database". NeuroImage 2011, 56, 766–781. [CrossRef]

[35] Wolz, R.; Julkunen, V.; Koikkalainen, J.; Niskanen, E.; Zhang, D.P.; Rueckert, D.; Soininen, H.; Lötjönen, J.M.P.; "The Alzheimer's Disease Neuroimaging Initiative. Multi-Method Analysis of MRI Images in Early Diagnostics of Alzheimer's Disease". PLoS ONE 2011, 6, e25446. [CrossRef] [PubMed]

[36] Braak, H.; Braak, E. "Staging of alzheimer's disease-related neurofibrillary changes". Neurobiol. Aging 1995, 16, 271–278. [CrossRef]

[37] Dubois, B.; Feldman, H.H.; Jacova, C.; DeKosky, S.T.; Barberger-Gateau, P.; Cummings, J.; Delacourte, A.; Galasko, U.; Gauthier, S.; Jicha, G.; et al. Research criteria for the diagnosis of Alzheimer's disease: Revising the NINCDS–ADRDA criteria. Lancet Neurol. 2007, 6, 734–746. [CrossRef]

[38] T. Shi, N. Boutry, Y. Xu, T. Géraud," Local intensity order transformation for robust curvilinear object segmentation", IEEE Transactions on Image Processing 31 (2022) 2557–2569

[39] D. Nie et al., "Fully convolutional networks for multi-modality isointense infant brain image segmentation", Procedding of the 2016 IEEE International Symposium on Biomedical Imaging (ISBI), pp. 1342-1345, 2016.

[40] T. Shi, N. Boutry, Y. Xu, T. Géraud, "Local intensity order transformation for robust curvilinear object segmentation", IEEE Transactions on Image Processing 31 (2022) 2557–2569.

[41] K. Acharya, D. Ghoshal, "Central moment and multinomial based sub image clipped histogram equalization for image enhancement", International Journal of Image, Graphics and Signal Processing (IJIGSP) 13 (1) (2021) 1–12

[42] M. Zhu, K. Zeng, G. Lin, Y. Gong, T. Hao, K. Wattanachote, X. Luo, "Iternet++: An improved model for retinal image segmentation by curvelet enhancing, guided filtering, offline hard-sample mining, and test-time augmenting", IET Image Processing (2022).